IN ROD

Electroplat d Chromium (EHC) is usually employed in applicat nder severe operating condition. Its mechanica hemical features allow its use in high temperatur vironments subjected to wear and exposed to sive agents.

EHC requir use of hexavalent Cr [1] [2] [3], however, the increas areness of its toxicity, compelled the imposition es for the wastewater treatments and for the wo exposure [4]. Additionally, it has to be considered the increasing demand of recycling solutions, w equired the increment of the component life and suc ely an easier and eco-friendly disposal. Considerin complex and severe environments, to replace EH innovative solutions considered in this work are a roplated double layer nickel chromium and differ hermal sprayed ceramic coatings, specifically gsten carbide in cobalt or cobalt chromium matrix. Two different thermal sprayed techniques are also

Starting from the failure analysis of existing hard chromium coatings, the failure conditions and the mechanism of failure were individuated. Based on this analysis, a proper experimental procedure was designed to identify the main as-deposited coating properties, thus being a reference for the selected innovative ones. The properties and failure mechanisms of these alternative solutions, tested at the same conditions, were studied and compared to the EHC.

The experimental procedure adopted was defined considering the main physical and chemical severe conditions that the coating has to face (mechanical stresses, friction, temperature gradients and chemical corrosion) in the majority of its applications. In particular: coating mechanical properties such as hardness and

In the case of test samples, especially those already preliminary damaged, more accurate sample selection is required: samples from both visibly defected and non-defected regions are chosen to understand the failure mechanisms and characterize the properties of the coating during operations.

Detailed about the parameters used for the production of the samples are not available due to confidentiality reasons.

C

O I EM

Visual characterization was carried out with Light Optical Microscopy (LOM) ("Nikon eclipse LV150NL") and Scanning Electron Microscopy (SEM) ("Zeiss evo 50"). Visual characterization was performed to measure the coating thickness and to characterize the coating morphology.

It was possible to estimate the grain dimensions in the copper substrate with the line method by image analysis on micrographs of etched samples with an acid solution prepared as 5 g $FeCl_3$, 50 ml HCl, 10 ml HNO_3 and 100 ml H_2O.

Chemical composition analysis was also performed with the Energy Dispersive X-ray (EDX) spectroscopy to aid the identification of the ceramic coating phases and the contamination from the liquid metal contact.

H (ISO 6507)

Vickers microhardness measurements were conducted with different parameters for each region of the samples. The load employed for the copper substrate was 100 gf, while for the coating cross section a load of 300 gf was used, due to the presence of very thin coatings.

A (ISO 2819 - EN 1071 ISO 27307)

Transversal scratch test evaluates the adhesion of the coating by measuring its critical load (i.e. the load that causes crack to form starting from the interface substrate-coating). If cracks develop inside the coating, the cohesive strength is smaller than adhesive strength.

The transversal scratch test machine used is the "CSM instruments Micro-combi tester" and the testing conditions for all samples were at constant load, at speed of 1.2 mm/min, a scratch length of 2 mm, and a Rockwell diamond-type indenter with a radius of 200 µm. Statistical evaluation was performed, when possible, using a 66% probability, indicating the presence of cracks in 2 out of 3 tests at the same load.

Wear testing was conducted to measure the friction coefficient and to qualitatively evaluate the behaviour of coatings at 200 °C. The linear test was performed with the "Rtec instruments Multifunction Tribometer MFT 5000" with an alumina ball of 6 mm as pin. Test duration was set at 12 minutes with a frequency of 15 Hz and a track length of 6.835 mm, resulting in a linear velocity of approximately 0.21 m/s.

M

It is widely reported that zinc and sulphur diffusion in copper substrate through damaged coating leads to the formation of fragile intermetallic alloys that causes the deterioration of the entire coating. Samples with dimensions (HxWxD) 1.5x1.5x0.5 cm were prepared and immersed in molten zinc. After 4 hours they were extracted and prepared for a visual and chemical analysis.

RE L AND DI C ION

The sample Cr90N shows the typical structure of EHC coatings [4] [6] as well as the sample Cr140FC, even though visibly damaged due to the service conditions at which it was subjected before being analysed.

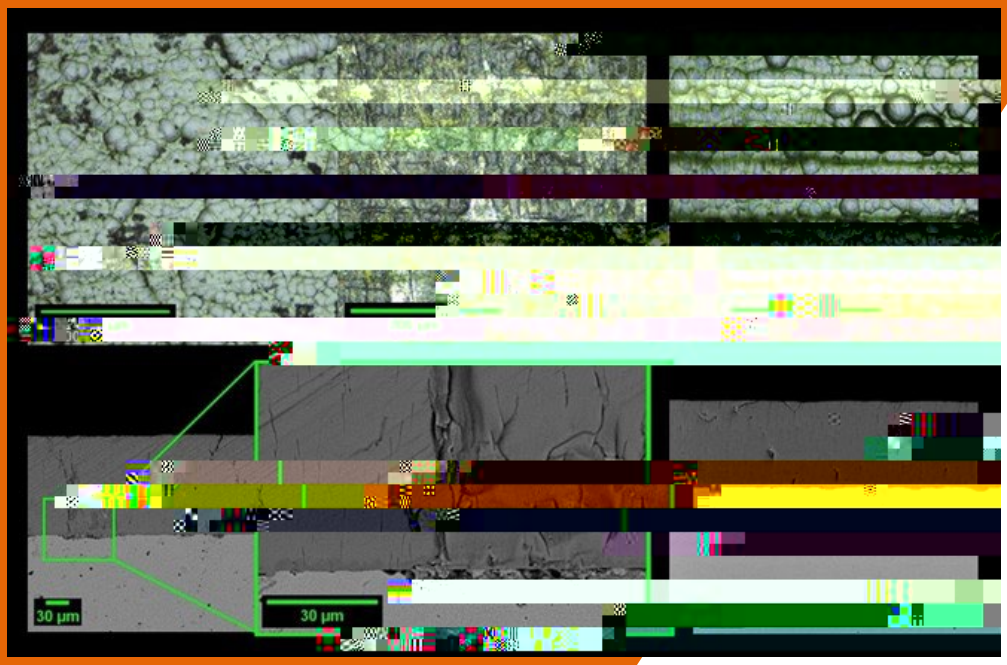

Fig.1 - Surface and cross section of EHC coatings: Cr140FC on the left and Cr90N on the right.

As can be seen in Fig.1, the coating surface of Cr140FC have the typical cracks of the EHC, moreover scratches and abraded zones are also visible. Transversal cracks along the entire coating thickness are visible in the cross section of the sample, while these are reduced in Cr90N. The average values of the mechanical test results are reported in the Tab.2.

Tab.2 - Mechanical test results: hardness and adhesion.

Sample	Coating hardness	Substrate hardness	Critical Load
Cr90N	892.0	108.8	12
Cr140FC	749.6	95.8	26

Since metallic elements not belonging to the nominal composition of the materials were individuated inside the transversal cracks of Cr140FC (see Fig.2), a zinc test was performed on both samples. In both samples delamination was observed after immersion in the molten metal, as can be observed in Fig.3.

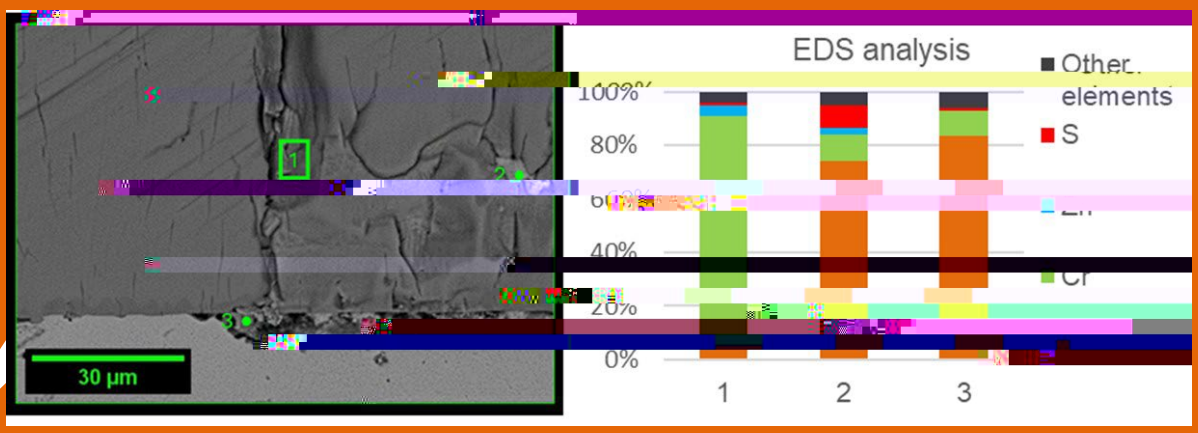

Fig.2 - Coating defect of sample Cr140FC (left) and EDX analysis of the infiltrated elements.

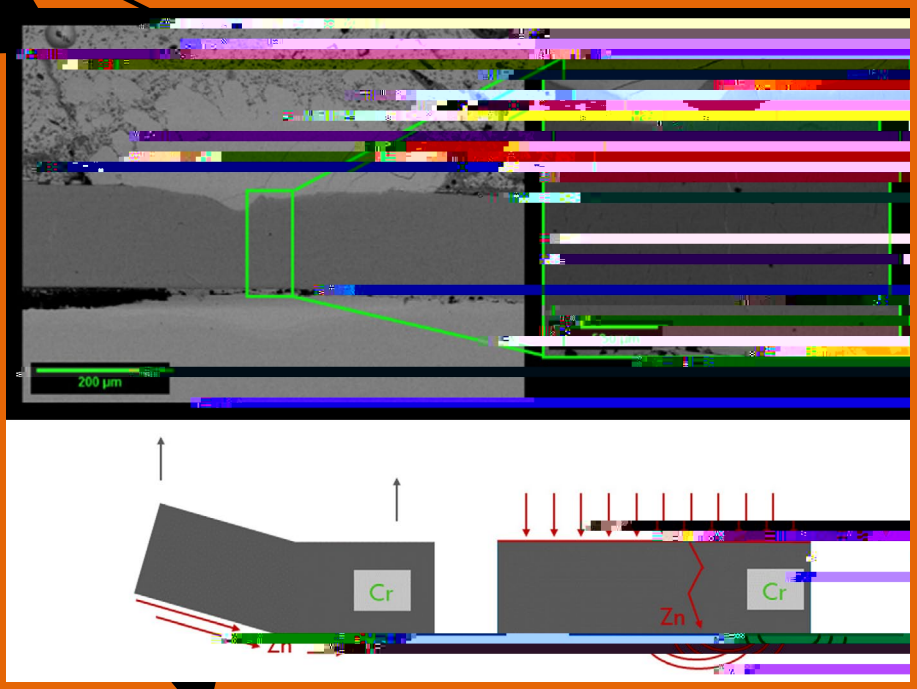

Fig.3 - SEM images and scheme of the infiltration mechanism of Zn for the EHC coating.

Cr90N has lower thickness compared to Cr140FC, however the coating and substrate hardness are higher: the latter is due to the presence of silver in the substrate, which improves the mechanical properties of the alloy with respect to pure copper.

Besides, the critical load of Cr90N is much lower than Cr140FC. This can be explained by the initial conditions: coating Cr was exposed to high temperature and to compressive stresses for a long period, which could have enhanced the chemical bond between coating and substrate.

From the results of the analysis on Cr140FC it was clear that infiltration of zinc and sulphur, with the subsequent formation of intermetallics with the copper substrate, was the principal cause of the coating failure together with the mechanical stresses leading to transversal cracks formation. These connect the substrate to the external part of the coating, thus hindering the shielding ability of the material.

The zinc test confirmed the coating failure mechanism: fragile copper based intermetallics containing mostly sulphur and zinc formed due to the molten metal penetration through the hard chromium microcracks and, they weakened the interface, finally leading to coating delamination owing to the pressure generated by the volume of liquid itself. In the case of Cr140FC, the effect of compressive and shear stresses on the surface during wear tests allowed a partial microcracks closure, thus delaying the infiltration of the molten metal and the consequent chemical attack mechanism.

C … EHC …

For the NiCr90N coating, micrographs in Fig.4 display the difference between the electrodeposited chromium and the electrodeposited nickel layers: the former features pores and microcracks, the latter is compact.

All thermal spray coatings showed thickness and composition inhomogeneities: the former is more evident for the HVOF WC-23CoN and for the samples with lower thickness, while the latter is present in all samples since it is an intrinsic characteristic of the deposition process. In particular, cobalt and chromium rich islands were detected.

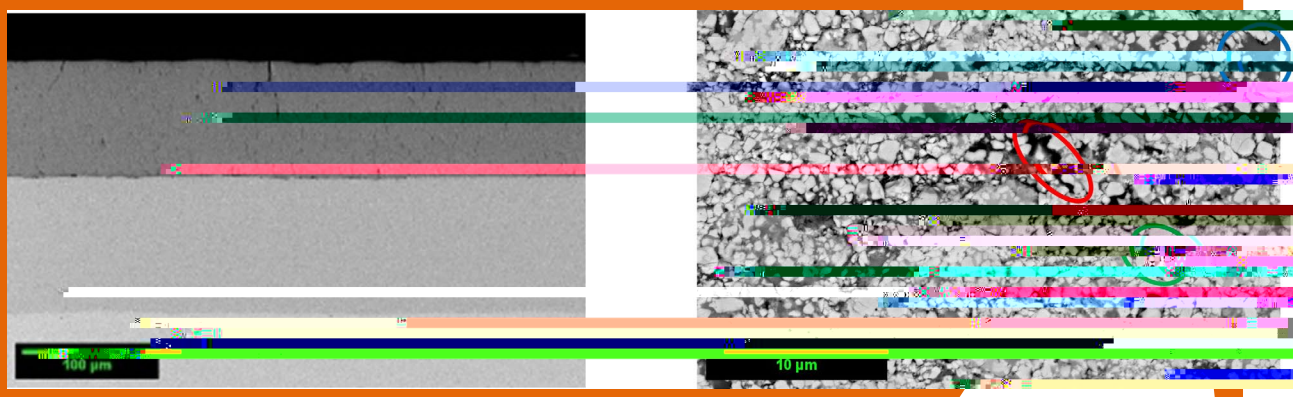

Fig.4 - NiCr90N double layer coating, from top to bottom: Cr layer, Ni layer and Cu substrate (left). WC-10Co5CrNgrad coating microstructure inhomogeneities, indicated by the red circle for Fe particles, blue for Co-rich and green for Cr-rich pools.

The difference in the compositions is reflected in the hardness values: even though WC-23CoN has a similar thickness to WC-11Co5CrNgrad middle and bottom sections and WC-10Co5CrNgrad bottom part, its hardness is slightly lower due to the reduced carbide fraction (Fig.5).Considering the three sections of WC-11Co5CrNgrad, it can be noticed an increasing thickness accompanied by a coherent trend in the coating and in the substrate hardness. Substrate of thicker thermal spray coatings are, in fact, subjected to high temperature and compressive stresses for a prolonged time, inducing recrystallization and plastic deformation at the surface, which is reflected on the average grain size at the interface coating-substrate (Fig.6). NiCr90N, WC-23CoN and WC-11Co5CrNgrad top have lower coating hardnesses, but they are still comparable to EHC.

It should also be noted that HVOF could be detrimental to the hardness of the coating, owing to the stronger decarburization effect on the WC fraction with respect to the HVAF process [7] [8].

Fig.5 - Coating cross section hardness comparison using a load of 300 gf.

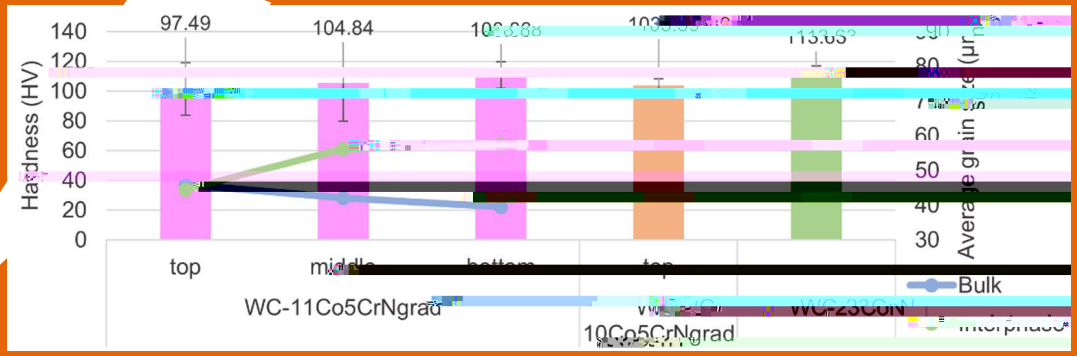

Fig.6 - Substrate hardness comparison using a load of 100 gf and corresponding average grain size for the sample WC-11Co5CrNgrad.

Thermal sprayed [illegible] showed a greater adhesion than EHC even though the bond between coating and substrate is physical and not chemical as in electrodeposition. The greater the thickness of the thermal sprayed coating the higher is the adhesion strength; indeed, thinner coating showed a very low adhesion, although it was still comparable to Cr90N and NiCr90N samples (Tab.3).

All samples showed a lower dynamic friction coefficient with respect to Cr90N, apart from WC-23CoN which showed a comparable value for the test at 5 N and a lower value at 7 N. Despite this, the material removal rate of all thermal spray coatings was almost negligible, the profilometry of the tracks were almost comparable to the surface roughness while for the electroplated coating a relevant depth was detected.

All thermal spray coatings showed an excellent to incipient corrosion with the exception of the thinner sample of

		Cr90N	NiCr90N	WC-23CoN	WC-11Co5CrNgrad			WC-10Co5CrNgrad	
					Top	Middle	Bottom	Top	Bottom
Critical load (N)		12	18	>30	<15	<25	>30	~15	~25
Friction coefficient	5 N	0.30	0.25	0.31	0.20	0.25	0.18	0.19	-
	7 N	0.44	0.24	0.32	0.26	0.29	0.22	0.21	-

cracking of the ceramic coating initiates at the surface. Consequently, stressed copper was then “extruded” and attacked by detrimental elements, mainly sulphur and traces of zinc.

Successively, crack opening and penetration of metals under the coating in the weak spots occurred, leading to coating delamination caused by weak interphases and mechanical forces at the surface, as well as cohesion failure and erosion.

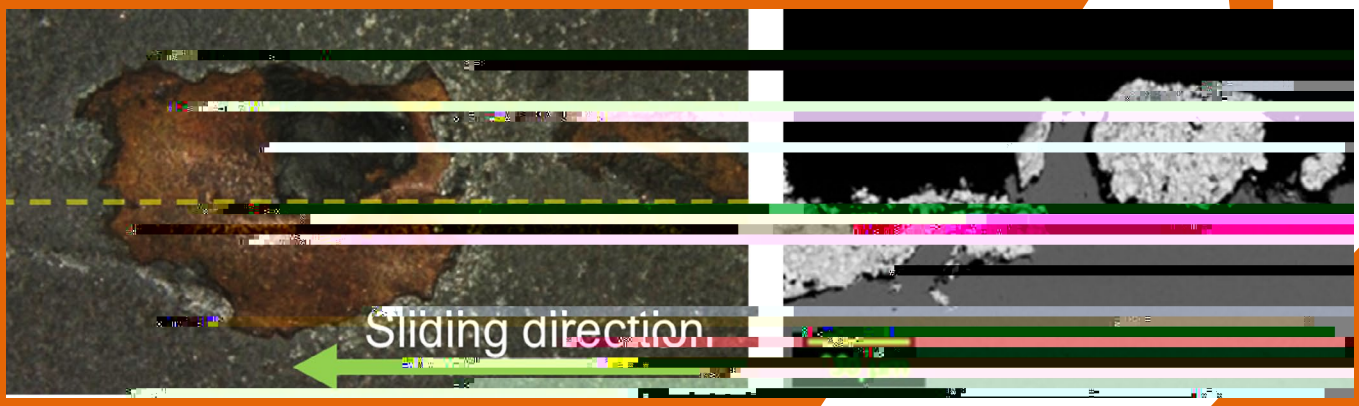

Fig.8 - WC-Co-HVAFused defect (left). Detail of defect cross section (right).

Differently from the WC-Co-HVAFused, WC-25CoD and WC-23CoU had a different mechanism of failure owing to their higher thickness.

These two samples do not show localized defects but extended erosion, coating surface cracks and depletion in the most stressed region. The depletion zone is higher in the WC-23CoU sample with respect to the WC-25CoD. The samples have different substrates: WC-25CoD features copper with chromium and zirconia particles, which is reflected in the higher hardness (110 HV instead of 94 HV), as opposed to WC-23CoU that comprises pure copper. This difference may be the cause of the earlier failure.

For both samples the adhesion strength is higher than 30 N.

Due to surface cracks, slag elements were able to penetrate through the coating and react with the substrate. Both samples showed presence of cracks also in the substrate, in particular WC-25CoD shows deeper average cracks (~3.1 mm instead of ~0.5 mm) owing to its prolonged usage time (triple than WC-23CoU).

In all cases zinc contamination of the crack edges is present.

CONCL ION

The analysis of hard chromium coatings (Cr140D and WC-23CoN) identified chemical corrosion as the main failure cause, owing to reaction with zinc and sulphur penetrating the coatings through microcracks. Delamination and substrate damage resulted from the formation of intermetallic alloys at the interface. Different innovative coatings exhibited varying levels of protection.

Double layer coating represents a valid alternative to the single layer, since the substrate is protected by the zinc layer, however frequent repairs would be needed and the hexavalent chromium problem would not be solved.

Ceramic coatings represent a promising alternative. The study emphasized the importance of thickness and composition, highlighting challenges such as thermal sensitivity and fragility during sample preparation. Besides also the characteristics of the substrate influences failures. Failures in WC-25CoD and WC-23CoU coatings were attributed to friction-induced depressions in the most stressed region, while WC-Co-HVAFused low thickness led to localized substrate deformation.

Adjusting the thickness and toughness of thermal sprayed cermet coatings is essential for their use in severe wear and temperature environments. Further research is needed to optimize the coating composition and to limit the costs for high thickness.

AKNOLEGMEN

Thanks to college Sina Sedaghatnezhad for the analysis of samples WC-23CoN and WC-23CoU.

REFERENCE

[1] formla[illegible]ectroplating 101: How Metal Plating Works.” Accessed: Jun. 17, 2023. [Online]. Available: https://formlabs.com/blog/electroplating-metal-plating/

[2] Vaisha[illegible] Mi[illegible]l (UC Davis), “Electroplating,” LibreTexts chemistry. Accessed: Jun. 17, 2023. [Online]. Available: https://chem.libretexts.org/Bookshelves/Analytical_Chemistry/Supplemental_Modules_(Analytical_Chemistry)/Electrochemistry/Electrolytic_Cells/Electroplating

[3] Luca M[illegible]agnin, “Chromium Plating.” 2020.

[4]